Research on the Change of Sulfur Dioxide Mass Concentration in Jilin Province, China

Xudong Zou[1,2,3]*, Rongping Li[1,3]**, Fu Cai[1,3], Nan Mi[1,3], Xiaoying Wang[1,3], Zhina Bai[4], Hujia Zhao[1], Yuche Liu[1], Rihong Wen[1], Ruiqiang Ding[5], Bo Hu[6], Qiong Wu[7], Hongyu Wang[1,3]

[1]Shenyang Institute of Agricultural and Ecological Meteorology, Chinese Academy of Meteorological Sciences, Shenyang 110166, China
[2]Northeast Geological S&T Innovation Center of China Geological Survey, Shenyang 110034, China
[3]Key Laboratory of Agrometeorological Disasters, Liaoning Province, Shenyang 110166, China
[4]Panjin Meteorological Service, Panjin 124000, China
[5]State Key Laboratory of Earth Surface Processes and Resource Ecology, Beijing Normal University, Beijing 100091, China.
[6]State Key Laboratory of Atmospheric Boundary Layer Physics and Atmospheric Chemistry, Institute of Atmospheric Physics, Chinese Academy of Sciences, Beijing 100029, China
[7]Panjin National Climate Observatory, Panjin 124010, China

Abstract

Using the monitoring data and meteorological data of SO_2 and other pollutants from nine cities in Jilin Province between 2016 and 2021, analyze the annual and monthly variations and spatial distribution of SO_2 concentrations across the province, as well as the related impacts from other environmental factors. The results showed that: (1) During the six-year period, no annual exceedance of the standard limit was observed in the entire province. There was a significant decrease in SO_2 concentrations across Jilin Province from 2016 to 2018. There were 5 days with excessive daily values in the whole province, all of which occurred in Baishan. Although SO_2 levels in the province remained low from 2019 to 2021, they were 16.0% and 22.2% higher than the national average in 2020 and 2021, respectively. According to the statistics of SO_2–24h–98, there were severe exceedances in the entire province from 2016 to 2017. The annual trends of relative humidity and wind speed are not conducive to reducing SO_2 concentrations, while the annual changes in precipitation and temperature have a favorable effect. The monthly average concentration of SO_2 across the province exhibits a "decreasing first and then increasing" trend. It is higher in January and December and reaches its lowest point in August. (2) The geographical distribution of SO_2 concentrations across the province shows high values centered in the southern and central regions, while low values are centered in the northern and eastern regions. It shows a zonal distribution from southeast to northwest. The spatial distribution of SO_2–24h–98 in the province

does not completely align with that of SO$_2$, and at times, the high-value center can be found in Tonghua, which is located in the southern part of the province. When comparing the similarity between spatial distributions, the correlation between terrain and SO$_2$ concentration is found to be higher, followed by GDP. (3) In comparison with other pollutants, SO$_2$ shows a positive correlation with PM$_{2.5}$, PM$_{10}$, CO, NO$_2$, and AQI, and a negative correlation with O$_3$. Among them, the correlation with PM$_{2.5}$ is the highest, with a correlation coefficient of 0.79. The impact of relative humidity on SO$_2$ varies significantly between the heating and non-heating periods. During the heating period, the SO$_2$ concentration first increases and then decreases with the increase in relative humidity, reaching a maximum average concentration of 26.1 μg·m^{-3} when the relative humidity is between 70% and 80% (inclusive). During the non-heating period, however, the concentration level remains relatively low. An analysis of energy consumption across the province over the past decade shows a significant decrease in coal consumption and an increase in electricity and natural gas consumption, while the proportion of oil products has increased by 2.1%.

Introduction

SO$_2$ is one of the major pollutants causing air pollution. In the atmosphere, sulfur dioxide can be oxidized to form sulfuric acid mist or sulfate aerosol, which is an important environmental acidification precursor. The impact of SO$_2$ on the environment mainly manifests in two aspects: Firstly, SO$_2$ forms sulfate aerosols with particle sizes less than 2.5 μm through gas-particle conversion, which is one of the main components of haze, reducing atmospheric visibility. High concentrations of SO$_2$ can seriously harm human health. Secondly, SO$_2$ and its oxidation products can combine with water molecules and fall to the ground in the form of wet deposition. This strongly acidic wet deposition can cause damage to natural ecosystems. In the atmospheric environment of urban areas, SO$_2$ mainly comes from primary emissions, such as the burning emissions of coal and high-sulfur gasoline and diesel [1, 2]. Due to the environmental hazards posed by SO$_2$, many countries, including China and the United States, have included SO$_2$ as one of the indicators to assess the quality of urban ambient air [3]. In previous research, data on SO$_2$ concentrations obtained through satellite detection and ground monitoring were used separately to analyze the changes and distribution of SO$_2$ concentrations in various regions, as well as the influencing factors. Additionally, predictions of SO$_2$ concentration changes and assessments of pollution risks were conducted. For example, satellite-observed SO$_2$ columns from 2005 to 2016 were employed, and a spatial econometric approach was applied to investigate the socio-economic factors influencing SO$_2$ pollution in 270 prefecture-level cities in China [4]. Based on the daily average concentration in Shandong Province from 2014 to 2019, the influence of the diurnal temperature range, secondary production, precipitation, wind speed, soot emission, sunshine duration, and urbanization rate on the SO$_2$ concentration is explored [5]. Both a model for assessing the population's relative risk of air pollution exposure and air pollution concentration methods were applied in a case study to determine the optimal method for evaluating the risk of population exposure to sulfur dioxide [6]. Monitoring data was used to analyze the changes in SO$_2$ concentration and spatial distribution patterns in Bali, Indonesia, from 2011 to 2020 [7]. Analyze the consistency of trends in observations of sulfur components in air and precipitation from major regional networks and estimates from six different global aerosol models from 1990 until 2015 [8]. Using ground, aircraft, and satellite measurement data, a ten-year (2004-2014) trend analysis of tropospheric SO$_2$ and aerosol pollution in Maryland, USA, was conducted [9].

Jilin Province is located in the central part of northeast China, occupying a geostrategic position at the heart of Northeast Asia. The province's terrain is characterized by higher elevations in the southeast and lower in the northwest, with the central and western regions boasting vast plains. The climate of Jilin Province is a temperate monsoon climate with pronounced continental characteristics. Summers are hot and rainy, while winters are cold, dry, and protracted. The average temperature in winter is below −11°C, while the average temperature in the plains during summer is above 23°C. Due to the severe cold winters and long heating seasons in Jilin Province, which typically begin in October and last until April of the following year, heating is predominantly coal-based. This has led to a noticeable seasonal pattern of air pollution in the province. Jilin Province holds a prominent position in China's industrial landscape, particularly in manufacturing automobiles and high-speed trains, at the leading domestic level. Jilin Province faces prominent structural contradictions in its energy sector, with coal consistently accounting for more than 70% of primary energy consumption, while the proportions of oil and natural gas are below the national average. As a traditional old industrial base, Jilin Province has experienced a certain degree of lag in atmospheric pollution prevention and control [10]. Since the implementation of the revitalization and development plan for Northeast China, the issue of air pollution in the region has become more severe due to the regional

economy's rapid development and energy consumption's rapid growth. The type of pollution has also gradually shifted from a single coal smoke pollution to a complex air pollution [11]. Air pollution control promotes green development and a circular economy, facilitating the optimization and upgrading of industrial structures and improving economic growth's quality and efficiency. It ensures people's lives and health while pursuing economic development. Currently, research on the long-term characteristics of SO_2 pollution in Jilin Province is relatively scarce. This paper utilizes statistical data, including monitoring data of SO_2 and other pollutants, meteorological data, and energy consumption, to analyze the spatio-temporal variation characteristics of SO_2 concentrations in Jilin Province over the past six years. The study explores the factors that influence natural and social activities associated with environmental changes. This study provides theoretical support for further understanding the status of air pollution in cities in Jilin Province and for carrying out governance measures.

Data and Methods

The monitoring data of SO_2 and other ground air pollutants (AQI, $PM_{2.5}$, PM_{10}, CO, NO_2, O_3) concentrations were sourced from the urban monitoring data of the Jilin Provincial Environmental Protection Bureau. The monitoring period covers January 1, 2016, to December 31, 2021. The daily evaluation index for SO_2 is the 24-hour average mass concentration, with the secondary concentration limit set at 150 μg•m^{-3}. The annual evaluation index of SO_2 is the average mass concentration throughout the year, and the secondary concentration limit is 60 μg•m^{-3}. The data statistics strictly follow the "Ambient air quality standards" (GB3095-2012) [12] and the "Technical regulation for ambient air quality assessment (on trial)" (HJ663-2013) [13]. The actual valid monitoring days for SO_2 mass concentration over six years in 9 cities across the province totaled 2,192 days, with no missing data, which meets the national evaluation technical specifications. The meteorological observation data were sourced from the China Meteorological Administration. Taking into full consideration the completeness and representativeness of the data, information from one meteorological observation station was adopted in each region. All data underwent rigorous quality control and inspection. The population, GDP, and vehicle ownership data for the entire province were sourced from the Jilin Provincial Bureau of Statistics. Topographical data were obtained from the Chinese National Basic Sciences Public Science Data Center, and the Jilin Provincial Environmental Protection Bureau provided data on energy consumption.

The correlation between SO_2 and other pollutants was analyzed using the Spearman correlation analysis in SPSS software. Spatial analysis of SO_2 concentration and other factors was conducted using ArcGIS software, with the Kriging interpolation method used for interpolation processing.

Temporal and Spatial Variation Characteristics of SO_2 Mass Concentration

Temporal Variation of SO_2 Mass Concentration

Interannual Variation of SO_2 Mass Concentration

A statistical comparison was conducted on the annual average changes and exceedances of SO_2 in nine cities across the province from 2016 to 2021 (see Fig. 1a). From 2016 to 2021, the annual average value of SO_2 in all nine cities did not reach 60 μg•m^{-3}, indicating no exceedances. During 2016-2017, the province-wide SO_2 concentrations were significantly high, with ranges of 4.7-73.8 μg•m^{-3} and 5.3-89.4 μg•m^{-3}, respectively, which were 1.8% and 13.9% higher than the national averages of 22 μg•m^{-3} and 18 μg•m^{-3}, respectively. Among them, the figure in 2017 decreased by 8.5% compared to the previous year. The average value of the whole province in 2018 decreased significantly by 36.1% compared with 2017. The range of variation in 2018 was 3.9-42.8 μg•m^{-3}, which was 6.4% lower than the national average of 14 μg•m^{-3}. Among the cities, Baishan, Tonghua, and Changchun had relatively high concentration values. The daily average exceedance standard is 150 μg•m^{-3}. Among the three years, only Baishan had daily exceedances, with 3 days in 2016 and 2 days in 2017, while no other daily exceedances were observed.

From 2019 to 2021, the province's SO_2 levels remained low, with ranges of 4.1-32.1 μg•m^{-3}, 5.4-35.1 μg•m^{-3}, and 6.1-26.0 μg•m^{-3}, respectively. Compared to the previous year, the average values decreased by 18.3%, increased by 8.4%, and decreased by 5.2%, respectively. Respectively, they were 2.7% lower, 16.0% higher, and 22.2% higher than the national averages of 11 μg•m^{-3}, 10 μg•m^{-3}, and 9 μg•m^{-3}. During these three years, only Tonghua showed a continuous increase in annual average concentration values, while the other cities remained flat or decreased slightly, with no daily exceedances observed.

Although the annual average SO_2 concentration values in the province did not exceed the standard during the six years, the statistical SO_2–24h–98 showed severe exceedances in 2016-2017 (see Fig. 1b), with exceedances observed in all cities except Baicheng and Yanbian. In 2018, the SO_2–24h–98 values in all cities decreased significantly, substantially reducing the number of cities exceeding the standard. Only Baishan exceeded the standard. The province's average SO_2–24h–98 also exceeded the standard in 2016-2017. The average SO_2–24h–98 in the province continued to decrease significantly in 2019. From 2019 to 2021, all cities' SO_2–24h–98 values remained low, with no exceedances observed. In 2016, the Jilin Provincial Government issued the "Clean Air Action Plan",
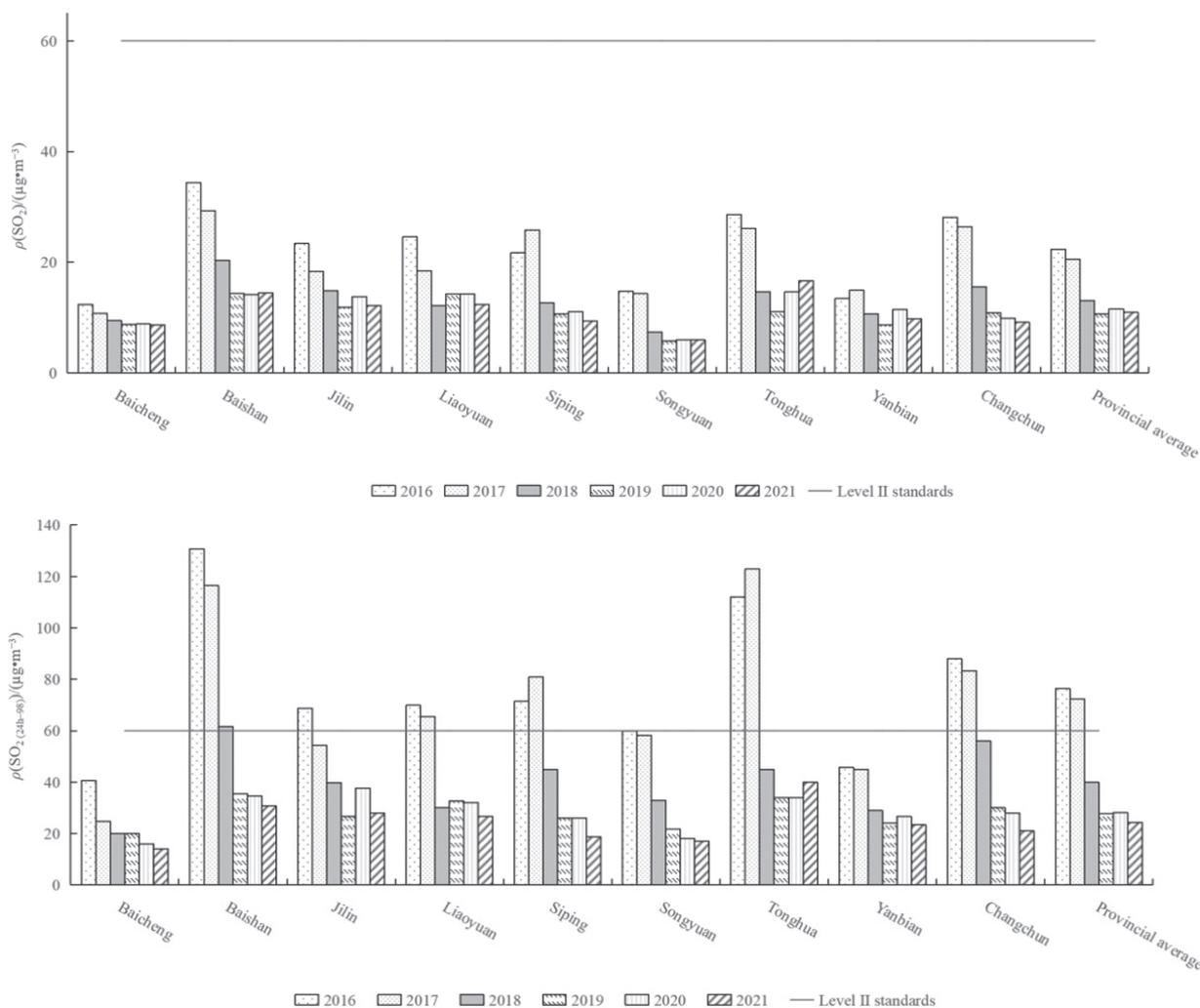
Fig. 1. Mass concentrations of SO$_2$ (a) and SO$_2$–24h–98 (b) in cities of Jilin Province from 2016 to 2021. The bar chart represents the average SO$_2$ concentration in each city per year, and the red horizontal line indicates the standard limit of SO$_2$ concentration.

targeting key regions, fields, and periods to vigorously tackle haze pollution. It was committed to winning the battle against air pollution prevention and control, gradually improving the ambient air quality throughout the province. Consequently, there was a significant decrease in SO$_2$ concentrations from 2016 to 2018, and the concentrations remained low after 2019.

Meteorological factors have a significant impact on air quality. Statistics on the annual average SO$_2$ mass concentrations, the number of days exceeding the standard limit, and a comparison with meteorological factors have been compiled for nine cities across the province from 2016 to 2021 (see Table 1 for details). The annual average SO$_2$ and SO$_2$–24h–98 concentrations across the province showed a downward trend from 2016 to 2021. After 2018, there were no days with SO$_2$ concentrations exceeding the standard limit in the entire province. From 2016 to 2021, the annual average temperature showed an upward trend, with the highest value occurring in 2019. The relative humidity first decreased and then increased, reaching its lowest value in 2019. Wind speed showed a slight downward trend;

precipitation increased from 2017 to 2020 but decreased in 2021. Increased temperature and rising wind speed are conducive to vertical convective motion of air [14]. Throughout the year, there is a positive correlation between relative humidity and SO$_2$ [15]. Precipitation has a mitigating effect on air pollution. Among the interannual variations of various meteorological factors, an increase in relative humidity and a decrease in wind speed are not conducive to reducing SO$_2$ concentrations, while an increase in precipitation and temperature has a beneficial effect on reducing SO$_2$ concentrations.

Seasonal Variations in SO$_2$ Mass Concentration

The average monthly mass concentration of SO$_2$ in Jilin Province from 2016 to 2021 showed a trend of "first decreasing and then increasing", with the range of concentration variations being larger in winter and smaller in summer (see Fig. 2a). The monthly average mass concentration of SO$_2$ gradually decreased from January to August, reaching its lowest value of 7.0 μg•m^{-3} in August. From September to January of the

Table 1. The table presents the annual average values of SO_2 concentration and meteorological conditions in Jilin Province from 2016 to 2021, including the province's annual precipitation, temperature, humidity, wind speed, annual average SO_2 concentration, and the number of days with SO_2 exceeding the standard limits.

Year	Average temperature t_{mean}/°C	Average relative humidity RH_{mean}/%	Average wind speed $v_{wind(mean)}$/ $(m \cdot s^{-1})$	Annual precipitation/ mm	Average SO_2 concentration $\rho(SO_2)$/ $(\mu g \cdot m^{-3})$	Average SO_2 concentration of SO_2–24h–98 $\rho(SO_{2(24h-98)})$/ $(\mu g \cdot m^{-3})$	Days of SO_2 exceeding the standard/%
2016	5.8	65.4^{+*}/ (2016.3.16– 2017.3.15)	2.5^{+*}/ (2016.3.16– 2017.3.15)	775.1	22.4^-	76.4^-	3
2017	5.9	62.4^-	2.5^+	583.0	20.5^+	72.4^-	2
2018	5.8	62.5^-	2.6^-	687.0	13.1^-	39.9^+	0
2019	6.7	60.8^-	2.5^+	695.8	10.7^+	27.8^+	0
2020	6.3	67.3^{+*}/ (2019.7.1– 2020.6.30)	2.4^{-*}/ (2019.7.1– 2020.6.30)	765.9	11.6^-	28.1^+	0
2021	6.4	68.2^{+*}/ (2021.3.8– 2022.3.7)	2.4^{+*}/ (2021.3.8– 2022.3.7)	688.4	11.0^-	24.4	0

Notes: "*" indicates the average value of the marked time period; "−" indicates greater than the actual value; "+" indicates less than the actual value.

following year, it showed a monthly increase, reaching its highest value of 32.8 μg•m^{-3} in January. The daily variation range of SO_2 concentration shows a gradual narrowing from January to May, remains low from June to September, and gradually expands from October to January of the following year. It can be seen that the concentration of SO_2 remains high during the entire winter period from October to April of the following year, with a correspondingly large range of concentration variations. In the past six years, there were only 5 days in the whole province where the SO_2 concentration exceeded the standard, specifically 3 days in December and 2 days in January. No daily exceedance of SO_2 concentration occurred in other months.

Comparing the monthly variations of various meteorological elements (see Fig. 2b), both temperature and precipitation exhibit a trend of "first increasing and then decreasing" throughout the year. The highest temperature occurs in July, reaching 24.3°C, while the lowest is in January, at −13.2°C. The maximum precipitation is recorded in August, 174.5 mm, and the minimum precipitation is in January, with only 3.7 mm. The monthly variations of relative humidity and wind speed exhibit opposite trends. The maximum relative humidity occurs in August, reaching 81.5%, while the minimum relative humidity is observed in April at 43.7%. On the other hand, the maximum wind speed is recorded in April at 3.3 m/s, and the minimum wind speed is observed in September at 2.1 m/s. Although the summer season is characterized by high relative humidity and low wind speeds, the abundant precipitation facilitates the deposition of

SO_2 pollution. Additionally, the high temperatures in summer lead to active local air turbulence, which is conducive to the diffusion and dilution of SO_2 pollution. Compared to spring and autumn, the low temperatures, low wind speeds, and relatively high relative humidity in winter are all unfavorable conditions for reducing SO_2 concentrations. Moreover, the limited precipitation during winter hinders the settling of pollutants and the decrease in SO_2 concentrations. These factors contribute to high pollution events during the winter season.

Geographic Distribution of SO_2 Mass Concentration

Analysis of the spatial and geographical changes in SO_2 concentrations in nine regions of Jilin Province from 2016 to 2021. The annual average SO_2 concentrations and the spatial distribution of SO_2–24h–98 in these nine regions have been obtained annually. In the analysis of the annual average SO_2 concentration changes (refer to Fig. 3), it is observed that there were no instances of annual average SO_2 concentrations exceeding the standard limits across the entire province. From 2016 to 2018, the SO_2 pollution in Jilin Province was characterized by high concentration centers in Baishan, Tonghua, and Changchun, with a gradual decrease in concentrations moving from southeast to northwest in a ring-like pattern. The lowest SO_2 concentrations were observed in Baicheng, Yanbian, and Songyuan. The high-value center in the southeast continued to decline, with Baishan decreasing continuously from 34.4 μg•m^{-3} to 20.3 μg•m^{-3}, a decrease of 41%; Tonghua dropped continuously from 28.6 μg•m^{-3} to 14.6 μg•m$^-$
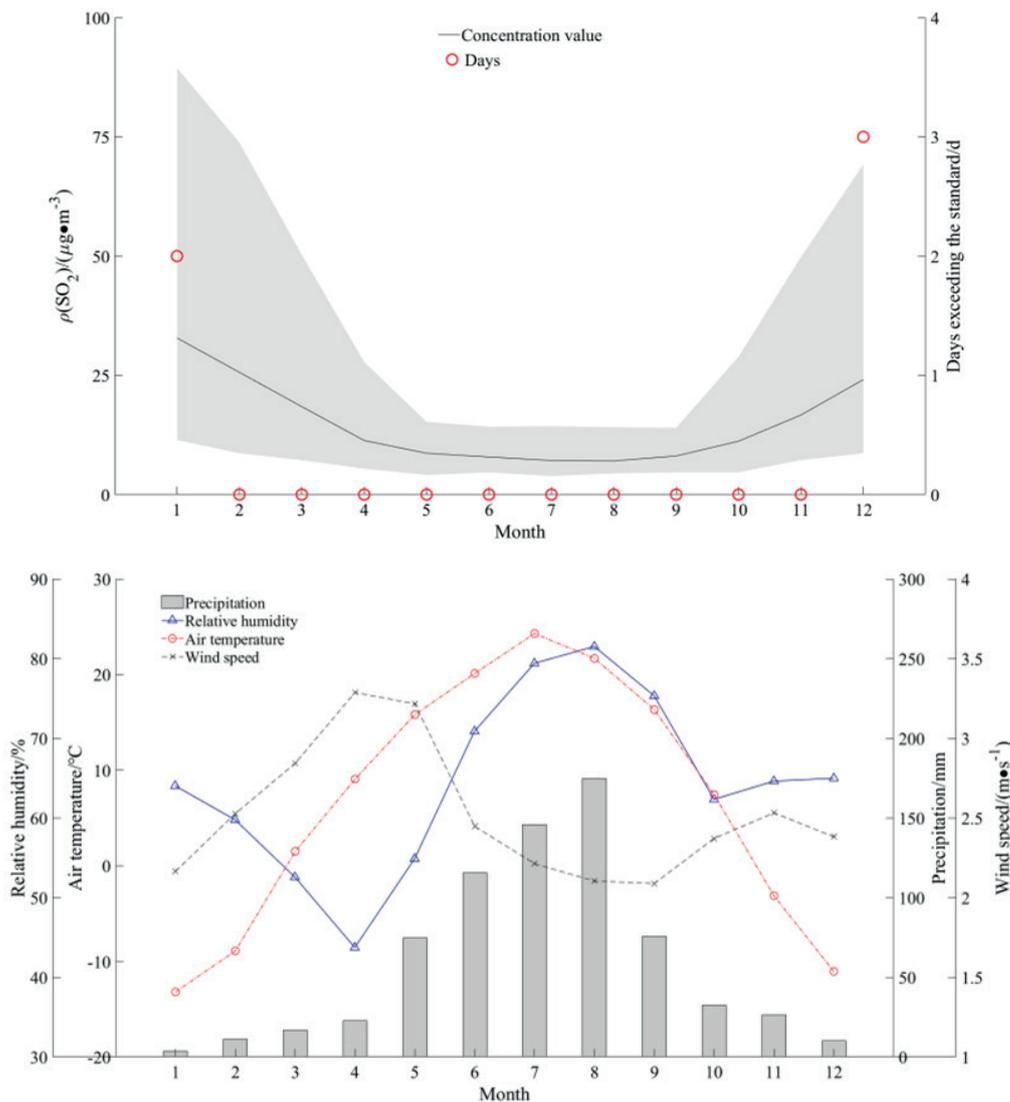
Fig. 2. Monthly distribution of average SO$_2$ mass concentration and number of days exceeding standards in Jilin Province from 2016 to 2021 (a), and average monthly variations of meteorological factors from 2016 to 2022 (b). In Fig. a, the red circles represent the number of days when SO$_2$ exceeded the standard, the black line indicates the average monthly SO$_2$ concentration across the province, and the shaded area depicts the range between the maximum and minimum daily average SO$_2$ concentrations observed within that month. In Fig. b, the bar graph represents precipitation, the solid blue line represents relative humidity, the dashed red line indicates temperature, and the dashed black line shows wind speed.

^{3}, a significant decrease of 49%; Changchun also experienced a continuous decline from 28.1 μg•m^{-3} to 15.5 μg•m^{-3}, a decrease of 45%. In the regions with lower values, Baicheng experienced a continuous decline from 12.4 μg•m^{-3} to 9.5 μg•m^{-3}, a decrease of 23%, while Songyuan saw a significant drop from 14.8 μg•m^{-3} to 7.4 μg•m^{-3}, a whopping 50% reduction. The difference between the high and low values decreased continuously from 22.0 μg•m^{-3} to 12.9 μg•m^{-3}, and the gap between the high and low values in the whole province decreased significantly.

From 2019 to 2021, the high-value centers across the province were in Baishan, Liaoyuan, and Tonghua, while the low-value centers were in Songyuan, Baicheng, and Yanbian. The overall trend in the province is still a ring-shaped decrease from southeast to northwest.

The area with concentrations higher than 10 μg•m^{-3} has shrunk significantly, with 7 cities exceeding this threshold in 2019 and only 5 cities in 2021. The average concentration in the province increased compared to the previous year, 2020, but decreased in 2021, and overall, it remains relatively stable. Specifically, Tonghua witnessed a continuous increase from 11.1 μg•m^{-3} to 16.7 μg•m^{-3}, representing a 50% increase. Cities like Jilin, Siping, and Yanbian showed a trend of first increasing and then decreasing in their respective concentrations, while other regions remained stable or showed slight decreases.

There are significant annual variations in the spatial distribution of SO$_2$–24h–98 across the province (see Fig. 4), with multiple cities exceeding the annual limit in 2016-2018. In 2016 and 2018, the distribution of SO$_2$
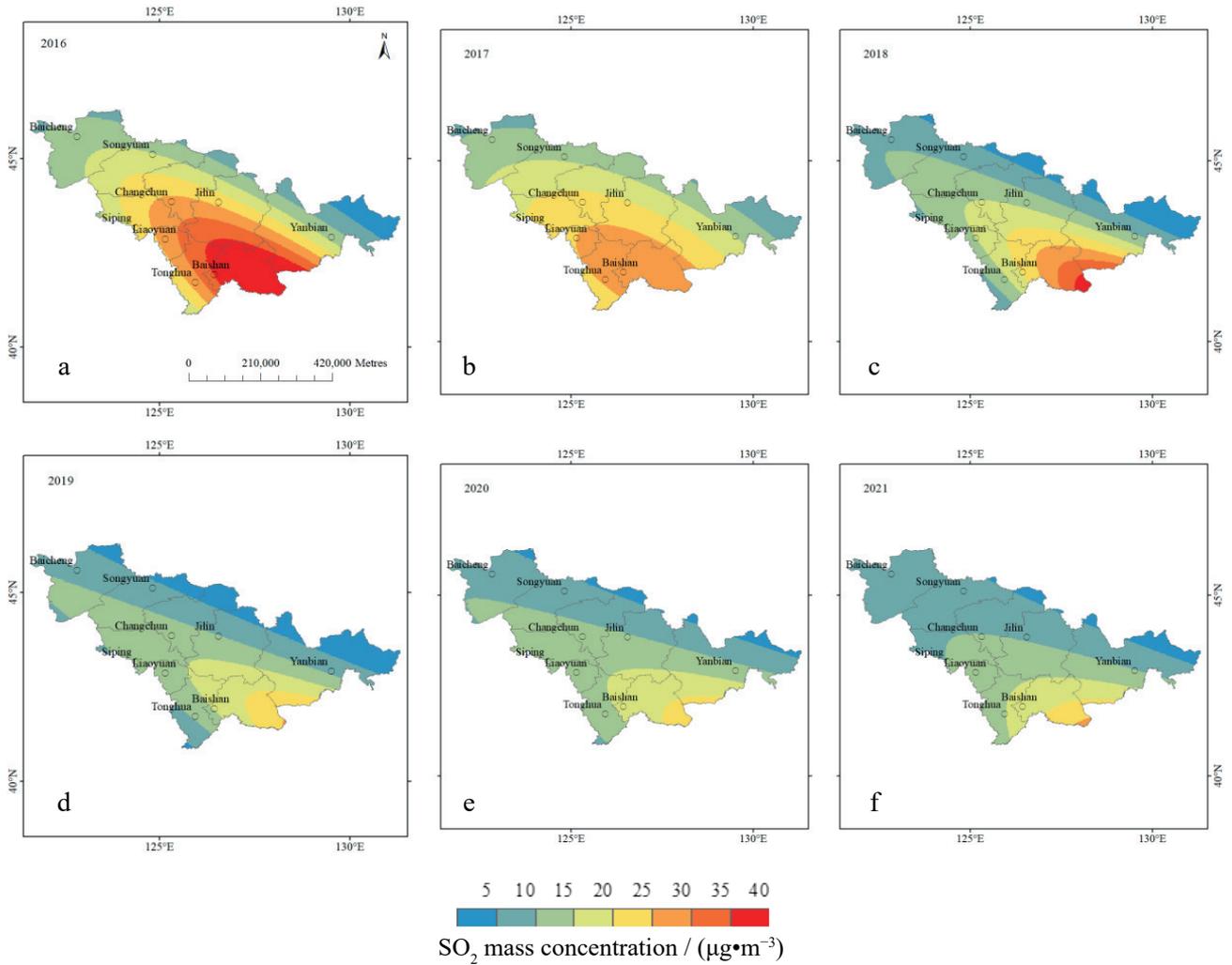
Fig. 3. A spatial change of $\rho(SO_2)$ in Jilin Province in 2016–2021. The different color bands represent the distribution of different SO_2 concentration ranges from 5 to 40 μg•m^{-3}.

Note: The base map is sourced from the Standard Map Service of the Ministry of Natural Resources of China [Approval No.: GS(2020)4619], with no modifications made to the boundaries. The same applies below.

across the province showed a ring-shaped decrease from southeast to northwest, while in 2017, the high-value center was located in Tonghua in the south, with a ring-shaped, stepped decrease towards the east and northwest, respectively. The annual exceedance of SO_2–24h–98 was very serious in 2016-2017, with 7 cities having SO_2–24h–98 values greater than 60 μg•m^{-3} in 2016, indicating an annual exceedance. Among them, Baishan, Tonghua, and Changchun had the highest SO_2–24h–98 values. In 2017, the number of cities with annual exceedances decreased to 5, with Tonghua, Baishan, and Changchun still having the highest SO_2–24h–98 values. In 2018, only Baishan had an SO_2–24h–98 value exceeding the 61.7 μg•m^{-3} limit. No other cities exceeded the limit.

From 2019 to 2021, all cities' SO_2–24h–98 values did not exceed the limit, and the province maintained a low level overall. In 2019, the range of SO_2–24h–98 values across the province was 20.0-35.4 μg•m^{-3}; in

2020, it was 16.0-37.7 μg•m^{-3}; and in 2021 it was 14.0-40.0 μg•m^{-3}. The area with SO_2–24h–98 values below 20 μg•m^{-3} gradually expanded, with only Baicheng having an SO_2–24h–98 value of 20 μg•m^{-3} in 2019, while Baicheng, Siping, and Songyuan all had values below 20 μg•m^{-3} in 2021.

The continuous growth in the number of vehicles, industrial structure, urban population, and human activities has led to the accumulation of SO_2 pollutants in urban areas [16, 17]. The spatial distribution of population, economy, number of vehicles, and terrain across the province is compared (see Fig. 5). The population distribution is characterized by high-value centers in central and western regions such as Changchun, Liaoyuan, and Siping, with an average population density exceeding 197 people per square kilometer. The values gradually decrease towards the south, north, and east, with Yanbian, Baishan, and Baicheng as low-value centers with a population density
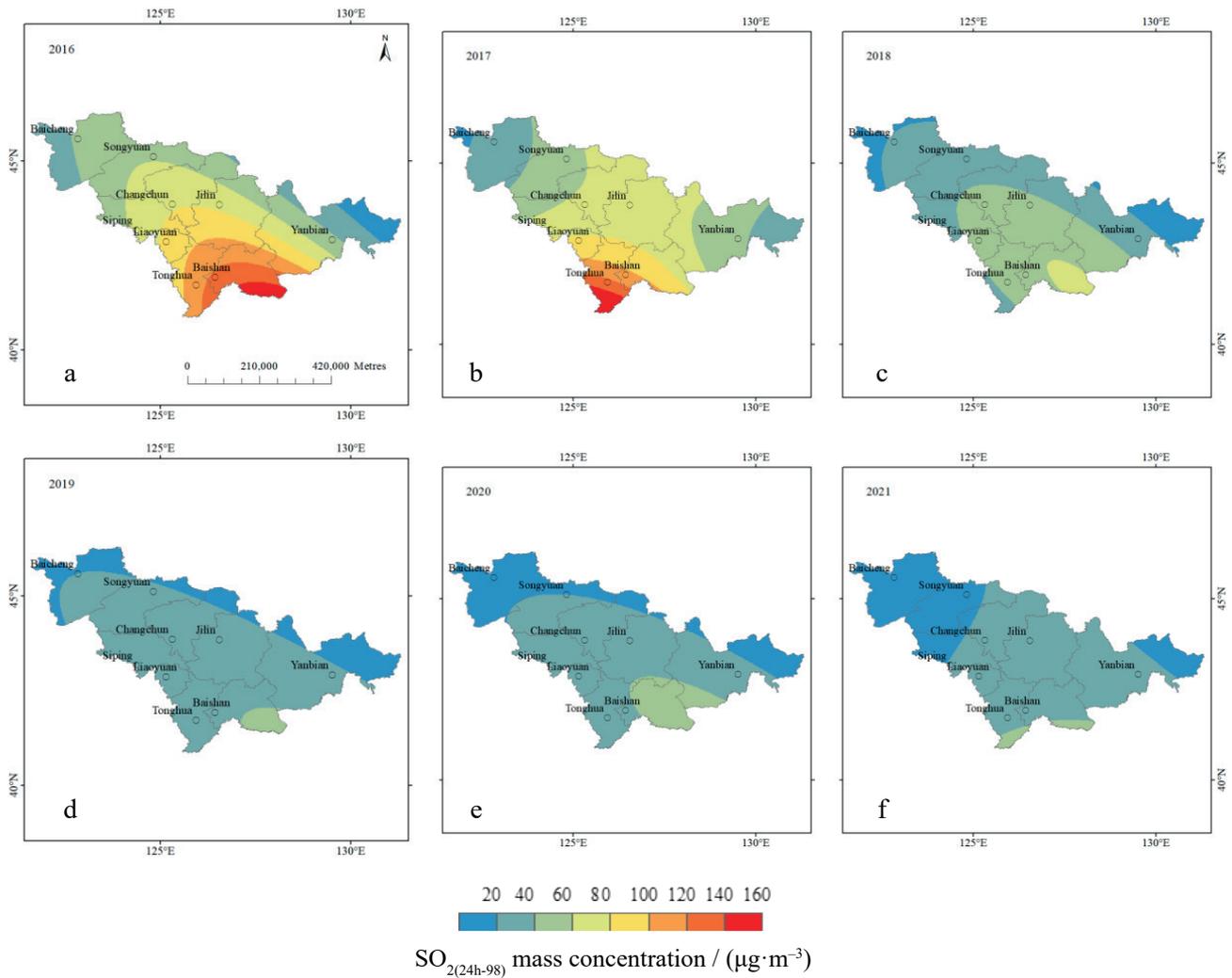
Fig. 4. A spatial change of $\rho(SO_{2(24h-98)})$ in Jilin Province in 2016–2021. Different color bands represent the geographical distribution of different $SO_{2(24h-98)}$ concentration ranges from 20 to 160 μg•m^{-3}.

of less than 74 people per square kilometer. High-value centers in central regions such as Changchun, Jilin, and Songyuan characterize the spatial distribution of economic output. Among them, Changchun has an average annual GDP of 657.3 billion yuan (accounting for 50.7% of the province), which is much higher than other regions. The values gradually decrease from the center to the periphery, with Liaoyuan, Baishan, and Baicheng as low-value centers, with GDPs below 56 billion yuan.

Cars significantly impact air pollution, and SO_2 is greatly affected by vehicle emissions [18, 19]. The regions with the largest number of vehicles are Changchun, Jilin, and Songyuan, which is consistent with the economic distribution. Among them, Changchun has 1.89 million vehicles (accounting for 41.9% of the province), far more than other regions. The regions with fewer vehicles are Baishan, Liaoyuan, and Tonghua, each having less than 250,000 vehicles. The number of vehicles gradually decreases from the high-value central region to the surrounding areas in the south and northwest. It is

noteworthy that the overall number of vehicles has been increasing year by year. The total number of vehicles in the province increased from 4.21 million in 2018 to 4.5 million in 2019 and then to 4.81 million in 2020, with an annual increase of approximately 300,000 vehicles. It can be seen that the development trend of the number of vehicles will have an adverse impact on SO_2 levels.

The high values of population, economy, and vehicle numbers in the province are concentrated in the central-west or central regions and gradually decrease towards the surrounding areas in a circular pattern. Unfavorable topographical conditions also contribute to SO_2 pollution [20]. The terrain of Jilin Province slopes from southeast to northwest, with a distinct characteristic of being high in the southeast and low in the northwest. With the central Daheishan Mountain as the boundary, it is divided into two major geomorphic regions: the eastern mountainous region and the central-western plain region. The highest elevation point is located in the Changbai Mountain range in the southeast, exceeding 2,600 meters. Baishan City, which is more seriously
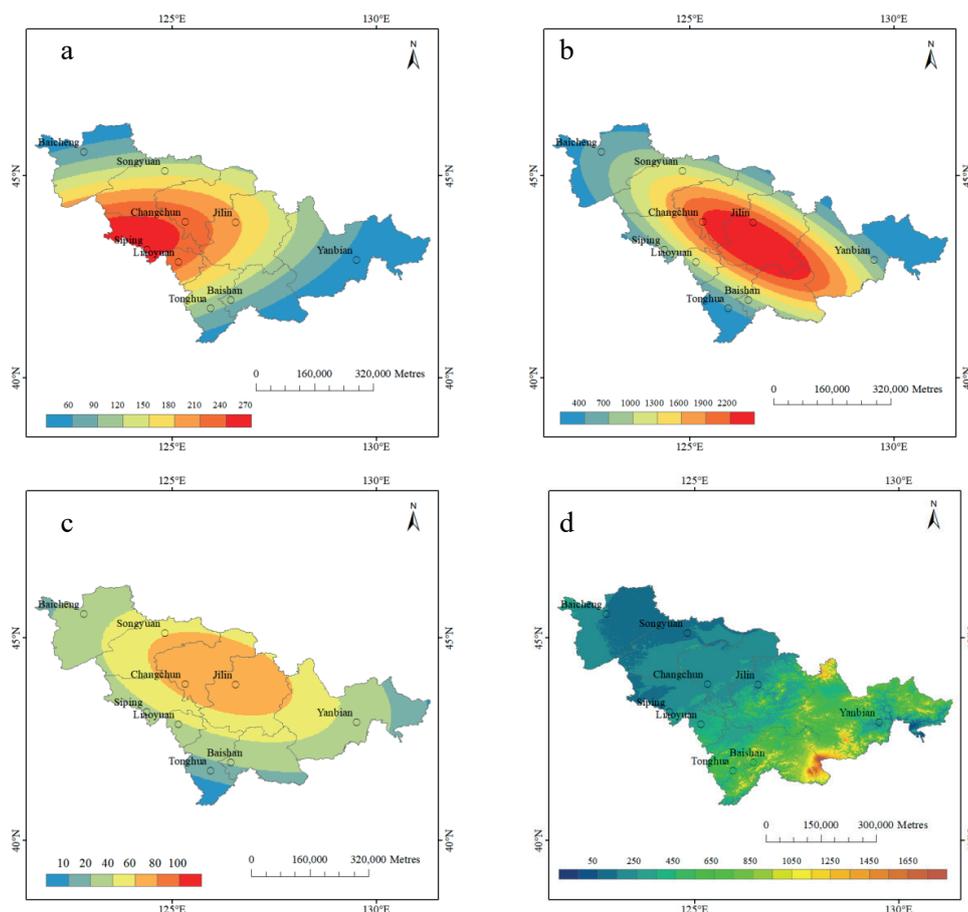
Fig. 5. The average population density, GDP, car ownership, and terrain of Jilin Province from 2018 to 2020 (a) population density/ (person•km^{-2}); (b) GDP/100 million yuan; (c) number of cars/10000; (d) terrain height/m). The different ranges of color band values represent the geographical distribution of population density, gross domestic product, number of cars, and terrain height across the province, respectively.

polluted, is located in the heartland of Changbai Mountain, with numerous mountains, rolling hills, and crisscrossed valleys. Tonghua City is also located in the Changbai Mountains, with over two-thirds of its territory covered by mountainous areas. Comparing the spatial distribution of population, economy, number of vehicles, and terrain, the spatial distribution of terrain and GDP across the province is relatively similar to that of SO$_2$ concentration values. In particular, the spatial distribution of terrain and SO$_2$ concentration values is more consistent. Overall, both show a pattern of high values centered in the southeast, gradually decreasing towards the northwest. This indicates that among the several factors being compared, SO$_2$ pollution is more significantly influenced by terrain, followed by GDP.

Correlation Between SO$_2$ and Other Environmental Factors

A correlation statistical analysis was conducted on the daily average concentrations of SO$_2$, PM$_{2.5}$, PM$_{10}$, CO, O$_3$, NO$_2$, and AQI across the province from 2016

to 2021, covering a total of 2192 days over the six-year period.

Correlation between SO$_2$ and PM$_{2.5}$, PM$_{10}$

The mass concentration of SO$_2$ shows a positive correlation with inhalable particulate matter (PM$_{2.5}$, PM$_{10}$) (See Fig. 6a and 6b). The correlation coefficients are 0.790 and 0.712, respectively, and both have passed the significance test at the two-sided 0.01 level. The correlation coefficient between PM$_{2.5}$ and SO$_2$ is higher than that of PM$_{10}$ and SO$_2$. The concentration of SO$_2$ increases as the haze intensifies [21]. SO$_2$ is an important gaseous precursor of PM$_{2.5}$, which can undergo photochemical reactions to produce SO$_4^{2-}$. Meanwhile, NO$_3^-$, SO$_4^{2-}$, and NH$_4^+$ are the most significant inorganic salts present in PM$_{2.5}$ [22]. Gaseous precursors such as SO$_2$ undergo homogeneous or heterogeneous reactions on the surface of particulate matter in the atmosphere, forming secondary particles such as sulfates and organic aerosols, which significantly impact the concentration of PM$_{2.5}$ [23]. Research has indicated that the correlation between PM$_{2.5}$ and pollutants such as CO, NO$_2$, and

SO_2 in urban atmospheres across China is significantly stronger than between PM_{10} and these pollutants [24].

Correlation Between SO_2 and CO, O_3

The mass concentration of SO2 is positively correlated with CO and negatively correlated with O_3 (see Fig. 6c and 6d). The correlation coefficients are 0.688 and −0.311, respectively, both of which have passed the significance test at the bilateral 0.01 level. The natural sources of CO pollutants in the atmosphere mainly include the oxidation of CH_4 and emissions from oceans and plants; anthropogenic sources are primarily the incomplete combustion of carbon-containing substances, such as motor vehicle exhaust, industrial production emissions, and deforestation [25, 26]. The annual variation in CO concentration is consistent with that of SO_2, both showing higher levels in winter and lower levels in summer. The high consumption of fuel and unfavorable meteorological conditions in winter contribute to the high pollution levels of CO [27]. When sunlight is strong, the OH radicals generated by the photolysis of O_3 cause SO_2 to gradually convert to sulfates, and both are simultaneously consumed [28]. The seasonal variation in SO_2 concentration is opposite to that of O_3. The monthly distribution of O_3 concentration shows higher values in summer and lower values in winter [29].

Correlation Between SO_2 and NO_2, AQI

Both the mass concentration of SO_2 and NO_2 and AQI show positive correlation (see Fig. 6e and 6f), with correlation coefficients of 0.733 and 0.484, respectively, both of which have passed the bilateral significance test at the 0.01 level. The correlation between SO_2 and NO_2 is second only to $PM_{2.5}$ and higher than other pollutants. Both of them come from combustion and industrial emissions. Both SO_2 and NO_2 have strong corrosive and physiological irritant effects. They are both precursors of acid rain and are also the main causes of atmospheric secondary pollution. Some studies have pointed out that SO_2 is most significantly affected by the heating period, during which NO_2 is also at a high level [30, 31].

Complex interactions, interplays, and interconversions exist among various components of atmospheric pollutants. AQI (Air Quality Index) simplifies the concentration of various air pollutants monitored routinely into a single conceptual index value, which can be used to represent the degree of air pollution at different levels and identify the primary pollutant. Correlation analysis related to AQI can reflect, to a certain extent, the proportion of pollutants in the comprehensive air pollution index. The correlation coefficient between SO_2 and AQI being less than 0.5 indicates that the correlation between the two is not strong. The correlation between SO_2 and AQI is lower than that of PM_{10}, $PM_{2.5}$, NO_2, and CO when they are compared.

Impact of Relative Humidity on SO_2

The impact of relative humidity on SO_2 is analyzed separately for the heating and non-heating periods (see Table 2). During the non-heating season, there is a significant decreasing relationship between relative humidity and SO_2 concentration. As relative humidity increases, the SO_2 concentration gradually decreases. When RH≤40%, the SO_2 concentration reaches its highest value of 9.3 μg•m^{-3}, and when RH>90%, the SO2 concentration drops to its lowest value of 6.9 μg•m^{-3}. During the non-heating period, the variation range of SO_2 concentration is relatively small, less than 2.4 μg•m^{-3}.

During the heating period, the SO_2 concentration first increases and then decreases with the increase of relative humidity, reaching a maximum average concentration of 26.1 μg•m^{-3} when the RH is between 70% and 80%. All days with excessive SO_2 levels over the 6-year period also occurred within the range of 60%<RH≤80%, with the highest number of excessive days (4 days) occurring when 70%<RH≤80%. The variation range of SO_2 concentration during the heating period is relatively large, reaching 12.6 μg•m^{-3}. This indicates that the impact of relative humidity on SO_2 differs between the heating and non-heating periods. The gradual increase in SO_2 concentration when RH≤80% suggests that an increase in relative humidity has an adverse effect on SO_2 pollution. Higher relative humidity is more conducive to forming particulate matter within a certain range of humidity, making it more likely to experience severe pollution under high humidity conditions [32]. When RH>80%, the SO_2 concentration decreases. Precipitation events often accompany high humidity conditions, and wet deposition can remove atmospheric pollutants [33].

Impact of Coal-fired Heating on SO_2 Emissions

China is the world's largest producer and consumer of coal, accounting for more than half of its energy mix [34]. The consumption of coal can reflect the amount of air pollution emissions. Jilin is a major province that relies heavily on coal for heating, with the heating season lasting approximately 6 months from October to April of the following year. It is evident that the high values of SO_2 occur predominantly during the heating period (see Fig. 7a). Over the six-year period, the range of the highest daily SO_2 concentrations during the heating season varied from 26.0 to 89.4 μg•m^{-3}, exhibiting a trend of decreasing year by year. The highest daily value occurred in January 2017, reaching a daily average of 89.4 μg•m^{-3}, while the lowest daily value was observed in February 2021, with a daily average of 26.0 μg•m^{-3}. The highest daily SO_2 concentrations occurred most frequently in January, followed by February and December. The lowest daily SO_2 concentrations during the heating season were similar across years, ranging from 6.0 to 9.2 μg•m^{-3}, and all occurred in October.
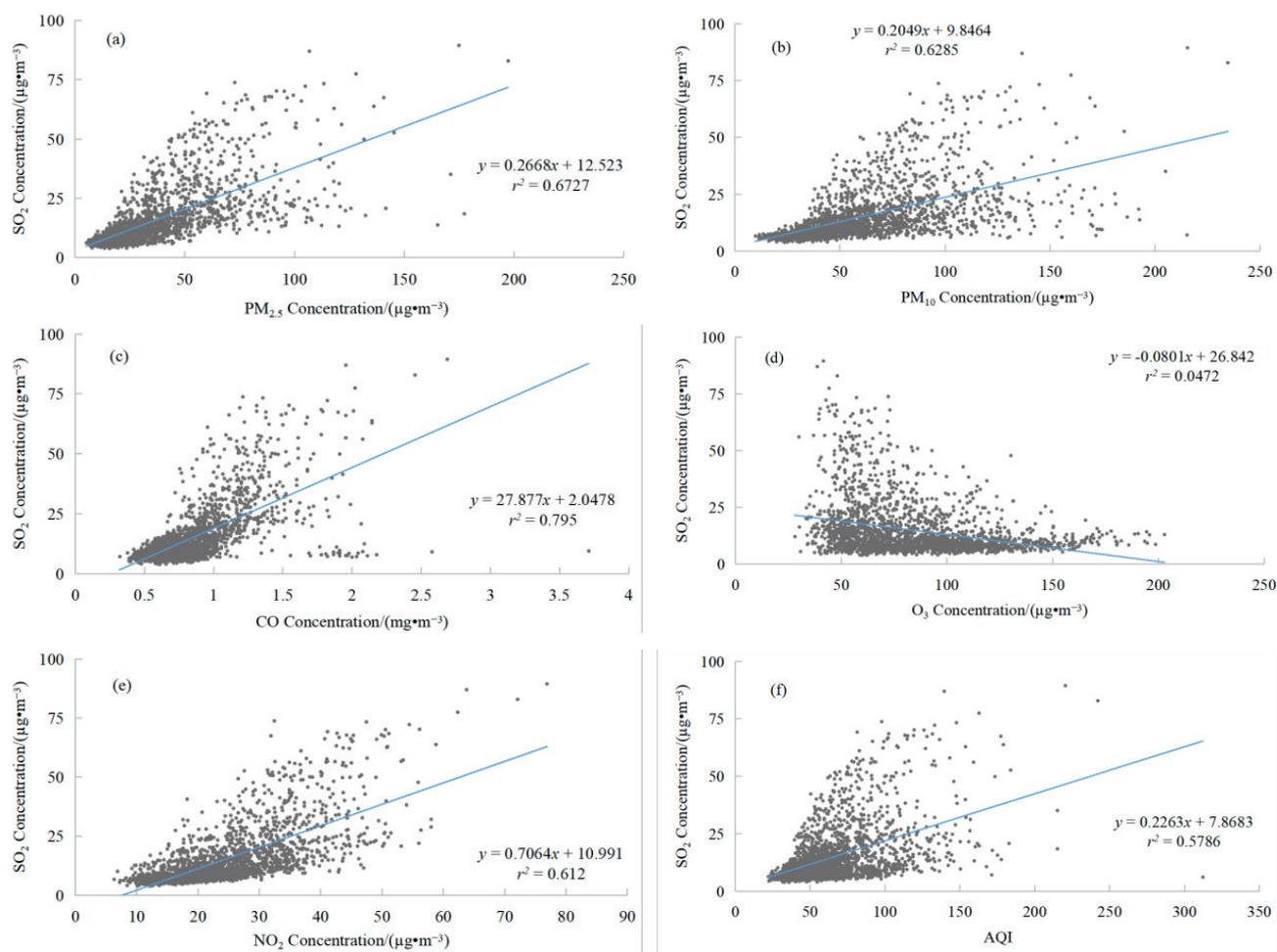
Fig. 6. Correlation analysis of SO$_2$ and PM$_{2.5}$, PM$_{10}$, CO, O$_3$, NO$_2$, AQI in Jilin Province in 2016—2021. The black dots represent the corresponding concentration values of SO$_2$ and various pollutants, while the blue straight line indicates the linear correlation between SO$_2$ and various pollutants.

Table 2. Mean concentration and days of SO$_2$ exceeding the standard under different relative humidity in Jilin Province in 2016–2021. The relative humidity ranges from 40% to 90% and is divided into equal intervals of 10%. The SO$_2$ mass concentration and the number of days with excessive SO$_2$ levels are statistically analyzed separately for the "heating period" and "non-heating period" corresponding to different relative humidity ranges.

Relative humidity (RH)/%	Days of monitoring/d	Mean value of ρ(SO$_2$)/(μg·m^{-3})	Days of SO$_2$ exceeding standard/d
rh≤40	1138/ 929	13.51/ 9.29	0/0
40<rh≤50	1223/ 683	17.04/ 8.93	0/0
50<rh≤60	1606/ 979	20.03/ 8.38	0/0
60<rh≤70	1782/ 1375	24.48/ 8.19	1/0
70<rh≤80	1393/ 2082	26.07/ 7.81	4/0
80<rh≤90	631/ 1803	23.10/ 7.32	0/0
rh>90	165/ 792	17.36/ 6.93	0/0

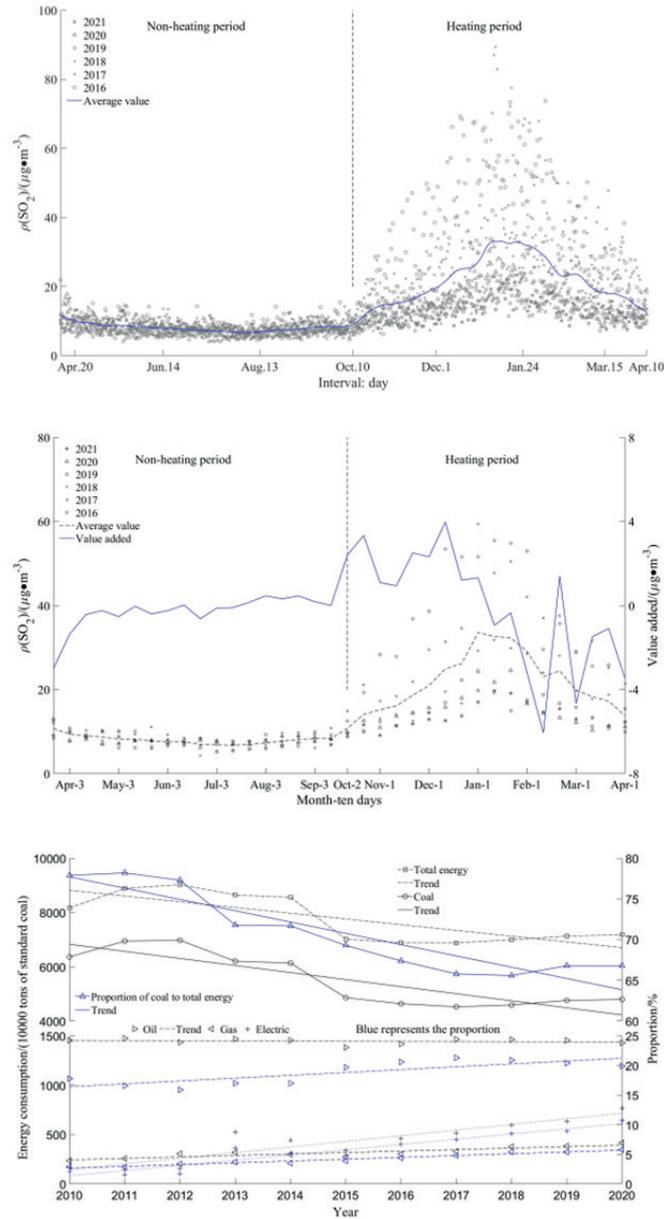Note: "/" means "heating period/non-heating period".

Fig. 7. Daily and ten-day changes of the SO$_2$ concentration in Jilin from 2016 to 2021 (Fig. a, Fig. b) and annual energy consumption change from 2010 to 2020 (Fig. c). In Fig. a, asterisks, triangles, squares, and other symbols represent the daily SO$_2$ mass concentrations for each year, respectively. The blue curve indicates the average value, and the non-heating and heating periods are on both sides of the vertical dashed line, respectively. In Fig. b, asterisks, triangles, squares, and other symbols represent the decadal values of SO$_2$ mass concentration for each month of each year, respectively. The black dashed curve indicates the average value, while the blue curve represents the variation in the monthly decadal values. The non-heating and heating periods are on both sides of the vertical dashed line, respectively. In Fig. c, squares, circles, left-pointing triangles, and other symbols represent the total energy consumption and the consumption values of individual energy sources, such as coal and oil, for each year, respectively. Blue symbols indicate the proportion of each energy source in the total energy consumption. Solid and dashed straight lines represent trend lines.

The average concentration of SO$_2$ during the heating period showed a continuous year-by-year decrease, from 35.9 μg•m^{-3} in 2016 to 13.7 μg•m^{-3} in 2021. During the non-heating period, the SO$_2$ concentration varied less significantly, with an average range of 6.7 to 9.4 μg•m^{-3} over the six years. The range of the highest daily SO$_2$ values during the non-heating period is 11.3—21.9 μg•m^{-3}, with most occurrences in April. The range of

the lowest daily value is 3.9—6.1 μg•m^{-3}, which occurs from April to August.

To analyze the annual variations in average SO$_2$ concentrations by dividing each month into early, middle, and late periods (see Fig. 7b). The range of daily maximum SO$_2$ concentrations during the heating period over a six-year period varies from 19.7 to 55.5 μg•m^{-3} from late December to late January. The range of the

lowest decadal concentration values per month varies from 8.8 to 14.9 μg•m⁻³, most occurring in mid-October. The decadal average value of SO$_2$ during the heating period has continuously decreased from 35.8 μg•m⁻³ in 2016 to 13.7 μg•m⁻³ in 2021, with an annual decline rate of up to 12.4%. During the non-heating period, the average decadal SO$_2$ concentration remains relatively stable, with the highest range of variation in decadal concentration values being 8.5 to 13.1 μg•m⁻³. The majority of these higher concentration values occur in mid-April. The lowest range of variation for the decadal SO$_2$ concentration is 4.3 to 6.9 μg•m⁻³, with the majority of these low values occurring from late June to early August. During the non-heating period, the average decadal SO$_2$ concentration varies relatively little, staying within the range of 6.7 to 9.4 μg•m⁻³. Throughout the year, significant increases in SO$_2$ concentration, exceeding 2.3 μg•m⁻³, are observed in mid-to-late October and late November to mid-December. These increases correspond to the periods when heating systems are initially turned on, with a notable drop in temperature. In early to mid-February, early March, and early to mid-April, there is a notable decrease in SO$_2$ concentration, with values dropping by more than −3.0 μg•m⁻³. These periods coincide with the cessation of heating systems and a significant temperature rise. These phenomena demonstrate that winter heating and rapid temperature fluctuations directly impact SO$_2$ pollution emissions.

Compare the trend of energy consumption in Jilin Province from 2010 to 2020 (see Fig. 7c). The overall energy consumption shows a decreasing trend, with an average of 86.96 million tonnes of standard coal from 2010 to 2012, and an average of 71.061 million tonnes from 2018 to 2020. Among them, coal accounts for the largest proportion of energy consumption, at 70.8%; oil products, natural gas, and electricity account for 18.8%, 4.2%, and 5.8% respectively. The proportion of coal in energy consumption has shown a continuous decline, while the proportions of electricity, natural gas, and oil have all shown an increase. The proportion of oil was 17.8% in 2010 and increased to 19.9% in 2020.

Conclusion

(1) From 2016 to 2018, the provincial average value continuously decreased and remained low from 2019 to 2021. Among them, all 5 days with excessive daily values from 2016 to 2017 occurred in Baishan. Although the annual average SO$_2$ concentration in the province did not exceed the standard limit during the six-year period, the statistical SO$_2$–24h–98 value showed serious exceedances from 2016 to 2018. In the interannual variability of various meteorological elements, an increase in relative humidity and a decrease in wind speed are detrimental to the reduction of SO$_2$ concentration, while an increase in precipitation and an increase in temperature play a beneficial role. The monthly average concentration of SO$_2$ exhibits a trend of "first decreasing and then increasing". It gradually decreases from January to August and then increases month by month from September to January of the following year. The range of concentration variation is also larger in winter and smaller in summer. The daily exceedance of the limit occurs in December and January, respectively. Among the monthly variations of various meteorological elements, summer precipitation and high temperatures are conducive to the settlement and dilution of SO$_2$. However, the low temperatures, low wind speeds, high relative humidity, and low precipitation in winter are all unfavorable factors contributing to the high pollution concentrations during this season.

(2) The spatial distribution of SO2 concentration across the province has high-value centers in Baishan, Tonghua, Changchun, and Liaoyuan and low-value centers in Songyuan, Baicheng, and Yanbian. Overall, it shows a circular decrease from southeast to northwest. The gap between high and low values across the province significantly narrowed between 2016 and 2018, but the reduction in the gap was not obvious thereafter. The spatial distribution of SO$_2$–24h–98 across the province does not completely align with the SO$_2$ concentration. In 2017 and 2021, high values of SO$_2$–24h–98 appeared in the southern region, while high values of SO$_2$ concentration were observed in the southeastern region. The spatial distribution of population, GDP, and car ownership across the province shows high values concentrated in the central-western or central regions, decreasing in a circular pattern towards the surrounding areas. The spatial distributions of topography, GDP, and SO$_2$ concentration values exhibit similarities, with the spatial distributions of topography and SO$_2$ being particularly consistent, both gradually decreasing from southeast to northwest. Tonghua and Baishan have the heaviest SO$_2$ pollution and are both located in complex, high-altitude mountainous areas. This suggests that topography has a greater influence on SO$_2$ pollution, followed by GDP.

(3) SO$_2$ is positively correlated with PM$_{2.5}$, PM$_{10}$, CO, and NO$_2$, respectively, with the highest correlation coefficient being 0.79 with PM$_{2.5}$. SO$_2$ negatively correlates with O$_3$, and their seasonal variations are opposite. The correlation between SO$_2$ and AQI is weaker than that of PM$_{10}$, PM$_{2.5}$, NO$_2$, and CO. The variation of SO$_2$ concentrations with different relative humidity is distinctly different between the heating and non-heating seasons. The range of SO$_2$ concentration changes during the heating season is much wider than during the non-heating season. During the non-heating season, the SO$_2$ concentration gradually decreases as the relative humidity increases, showing a significant decreasing relationship. However, during the heating season, the SO$_2$ concentration first increases and then decreases with relative humidity, reaching a maximum when the relative humidity is between 70% and 80% (inclusive), with an average concentration of 26.1 μg•m⁻³.

(4) A significant correlation exists between SO_2 concentrations and the heating season. The average concentration during the heating season is approximately 2.7 times that of the non-heating season. Over the course of six years, the highest concentration values most frequently occurred in January, followed closely by February. During the heating season, the average concentration of SO_2 has shown a consistent and significant decrease yearly. In the analysis of average concentrations by ten-day periods, there is a noticeable increase in SO_2 concentrations in the middle and late October, as well as from late November to mid-December. The increase exceeds 2.3 $\mu g \cdot m^{-3}$, corresponding to the start of heating and a sharp drop in temperature. Conversely, there is a significant decrease in SO_2 concentrations in early and mid-February, as well as early March. This corresponds to the cessation of heating and a substantial increase in temperature during the same period. This also indicates that SO_2 concentrations are directly affected by winter heating and rapid temperature changes. In the past decade, coal has accounted for the largest energy consumption in Jilin Province, at 70.8%, followed by oil products, electricity, and natural gas. The total energy consumption shows a downward trend, with a significant decrease in coal consumption and an increase in electricity and natural gas consumption. The proportion of coal in total energy consumption has also declined significantly, by 11 percentage points. Electricity has seen the largest increase in proportion, followed by natural gas. Although the consumption of oil products has declined slightly, its proportion in total energy consumption has increased by 2.1%.

Discussion

Although the concentration of SO_2 in the province showed a significant decline from 2016 to 2019, it did not continue to decrease between 2020-2021 but rebounded. Especially in 2021, it was 22.2% higher than the national average. The control and management of SO_2 emissions in Jilin Province need to be further strengthened. Although the annual SO_2 concentration values in the entire province did not exceed the standard, the statistical SO_2–24h–98 values showed severe exceedance from 2016 to 2018. This indicates that comprehensive consideration is needed when assessing the pollution status of SO_2.

When comparing the annual and monthly variations of various meteorological elements and SO_2 pollution, temperature, wind speed, and precipitation are negatively correlated with SO_2 concentration, while relative humidity is positively correlated with SO_2 concentration. Are the impacts of various meteorological conditions on SO_2 pollution completely consistent in different regions, and if not, what characteristics do they exhibit?

The province's population, economy, and number of vehicles are centered around Changchun, Jilin, Siping, and Liaoyuan, with high values located in the central region. However, the SO_2 pollution in the province decreases from the central and southern regions, with Baishan and Tonghua in the south and southeast as the centers, towards the surrounding areas in the middle and north. This demonstrates the influence of topography on air pollution, in addition to regional economics. When controlling SO_2 pollution, the impact of topography should be taken into consideration. The characteristics of meteorological conditions in complex topographical conditions and their impact on pollution are worth exploring.

When comparing different pollutants, how do their relationships vary with the seasons? Is the correlation between various pollutants consistent at different concentration levels? The correlation between relative humidity and SO_2 distinctly differs during heating and non-heating periods. Is this difference caused by variations in SO_2 concentration, differences in temperature backgrounds, or other reasons? In addition to local pollution source emissions, the impact of pollutant transport and migration from outside the region should also be considered. This study did not analyze this aspect, which is an area for future research to consider.

Coal and oil are traditional energy sources with heavy pollution emissions, while natural gas and electricity are cleaner. Over the past decade, coal consumption has declined significantly, while the proportion of natural gas and electricity consumption has increased markedly. Although oil consumption has declined, its proportion in total energy consumption has shown an upward trend, which is an area that needs to be controlled and improved in the future. After resolutely implementing the government's energy conservation and emission reduction policies, it is necessary to implement key supervision and governance in key emission areas to achieve the goal of long-term pollution control.

Acknowledgments

Funding

Conflict of Interest

The authors declare no conflict of interest.

References

1. AAS W., MORTIER A., BOWERSOX V., CHERIAN R., FALUVEGI G., FAGERLI H., HAND J., KLIMONT Z., GALY-LACAUX C., LEHMANN C.M.B., MYHRE C.L., MYHRE G., OLIVIÉ D., SATO K., QUAAS J., RAO P.S.P., SCHULZ M., SHINDELL D., SKEIE R.B., STEIN A., TAKEMURA T., TSYRO S., VET R., XU X.B. Global and regional trends of atmospheric sulfur. Scientific Reports, **9** (1), 953, **2019**.

2. GIOSANU D., MARIAN M.C., CONSTANTIN D. Air pollution meteorology. Case study: SO_2 and NO_2 monitoring in Argeș county. Current Trends in Natural Sciences, **10** (20), 72, **2021**.

3. KUTTIPPURATH J., PATEL V.K., PATHAK M., SINGH A. Improvements in SO_2 pollution in India: role of technology and environmental regulations. Environmental Science and Pollution Research, **29** (52), 78637, **2022**.

4. JIANG L., HE S.X., CUI Y.Z., ZHOU H.F., KONG H. Effects of the socio-economic influencing factors on SO_2 pollution in Chinese cities: A spatial econometric analysis based on satellite observed data. Journal of Environmental Management, **268**, 110667, **2020**.

5. WU H.S., HONG S., HU M.G., LI Y.H., YUN W.Z. Assessment of the factors influencing sulfur dioxide emissions in Shandong, China. Atmosphere, **13** (1), 142, **2022**.

6. DONG X.Y., ZHAO X.G., PENG F., WANG D.L. Population based air pollution exposure and its influence factors by Integrating air dispersion modeling with GIS spatial analysis. Scientific Reports, **10** (1), 479, **2020**.

7. RANAARIF S., YUWONO A.S. Analysis of the distribution of sulfur dioxide (SO_2) pollutant in Bali Island for the 2011-2020 period. IOP Conference Series: Earth and Environmental Science, **871**, 012031, **2021**.

8. AAS W., MORTIER A., BOWERSOX V., CHERIAN R., FALUVEGI G., FAGERLI H., HAND J., KLIMONT Z., GALY-LACAUX C., LEHMANN C.M.B., MYHRE C.L., MYHRE G., OLIVIÉ D., SATO K., QUAAS J., RAO P.S.P., SCHULZ M., SHINDELL D., SKEIE R.B., STEIN A., TAKEMURA T., TSYRO S., VET R., XU X.B. Global and regional trends of atmospheric sulfur. Scientific Reports, **9** (1), 953, **2019**.

9. HE H., VINNIKOV K.Y., LI C., KROTKOV N.A., JONGEWARD A.R., LI Z.Q., STEHR J.W., HAINS J.C., DICKERSON R.R. Response of SO_2 and particulate air pollution to local and regional emission controls: A case study in Maryland. Earth's Future, **4** (4), 94, **2016**.

10. CAI M. Research on the implementation of air pollution control policies in Jilin province. Changchun: Jilin University of Finance and Economics, China, pp. 1, **2020**.

11. LI Z.H. Study on the temporal and spatial variation characteristics of typical air pollutants sources in Jilin City. Jilin: Northeast Electric Power University, China, pp. 1, **2020**.

12. Ministry of Environmental Protection of the People's Republic of China. National standards of the people's republic of China: GB 3095-2012. Beijing: China Environmental Science Press, China, pp. 4, **2012**.

13. Ministry of Environmental Protection of the People's Republic of China. National environmental protection standards of the people's republic of China: Technical Specifications for Environmental Air Quality Assessment (Trial): HJ 663-2013. Beijing: China Environmental Science Press, China, pp. 2, **2013**.

14. ZHANG N., WANG Y. Mechanisms for the isolated convections triggered by the sea breeze front and the urban heat island. Meteorology and Atmospheric Physics, **133** (4), 1143, **2021**.

15. YANG H.M., PENG Q., ZHOU J., SONG G.J., GONG X.Q. The unidirectional causality influence of factors on $PM_{2.5}$ in Shenyang city of China. Scientific Reports, **10** (1), 8403, **2020**.

16. JION M.M.M.F., JANNAT J.N, MIA M.Y., ALI M.A., ISLAM M.S., IBRAHIM S.M., PAL S.C., ISLAM A., SARKER A., MALAFAIA G., BILAL M., ISLAM A.R.M.T. A critical review and prospect of NO_2 and SO_2 pollution over Asia: Hotspots, trends, and sources. Science of The Total Environment, **876**, 162851, **2023**.

17. WEI J., LI Z.Q., WANG J., LI C., GUPTA P., CRIBB M. Ground-level gaseous pollutants (NO_2, SO_2, and CO) in China: daily seamless mapping and spatiotemporal variations. Atmospheric Chemistry and Physics, **23** (2), 1511, **2023**.

18. KHREIS H., NIEUWENHUIJSEN M.J., ZIETSMANA J., RAMANIA T. Chapter 1 - Traffic-related air pollution: Emissions, human exposures, and health: An introduction. Traffic-Related Air Pollution, 1, **2020**.

19. FILIGRANA P., LEVY J.I., GAUTHIER J., BATTERMAN S., ADAR S.D. Health benefits from cleaner vehicles and increased active transportation in Seattle, Washington. Journal of Exposure Science and Environmental Epidemiology, **32** (4), 538, **2022**.

20. DANEK T., WEGLINSKA E., ZAREBA M. The influence of meteorological factors and terrain on air pollution concentration and migration: a geostatistical case study from Krakow, Poland. Scientific Reports, **12** (1), 11050, **2022**.

21. MA J.Z., CHU B.W., LIU J., LIU Y.C., ZHANG H.X., HE H. NO_x promotion of SO2 conversion to sulfate: An important mechanism for the occurrence of heavy haze during winter in Beijing. Environmental Pollution, **233**, 662, **2018**.

22. LIANG Y., JIANG H., LIU X.Z. Characteristics of atmospheric ammonia and its impacts on SNA formation in $PM_{2.5}$ of Nanchang, China. Atmospheric Pollution Research, **15** (4), 102059, **2024**.

23. LI H., MA Y.L., DUAN F.K., ZHU L.D., MA T., YANG S., XU Y.Z., LI F., HUANG T., KIMOTO T., ZHANG

Q.Q., TONG D., WU N.N., HU Y.X., HUO M.Y., ZHANG Q., GE X., GONG W.R., HE K.B. Stronger secondary pollution processes despite decrease in gaseous precursors: A comparative analysis of summer 2020 and 2019 in Beijing. Environmental Pollution, **279**, 116923, **2021**.

24. GUO H., GU X.F., MA G.X., SHI S.Y., WANG W.N., ZUO X., ZHANG X.C. Spatial and temporal variations of air quality and six air pollutants in China during 2015-2017. Scientific Reports, **9** (1), 15201, **2019**.

25. BYRNE B., LIU J.J., BOWMAN K.W., PASCOLINI-CAMPBELL M., CHATTERJEE A., PANDEY S., MIYAZAKI K., WERF G.R., WUNCH D., WENNBERG P.O., ROEHL C.M., SINHA S. Carbon emissions from the 2023 Canadian wildfires. Nature, **632**, 1, **2024**.

26. MANISALIDIS I., STAVROPOULOU E., STAVROPOULOS A., BEZIRTZOGLOU E. Environmental and health impacts of air pollution: A review. Frontiers in Public Health, **8**, 14, **2020**.

27. LIU Y.S., ZHOU Y., LU J.X. Exploring the relationship between air pollution and meteorological conditions in China under environmental governance. Scientific Reports, **10** (1), 14518, **2020**.

28. JIAO X.Y., HE C.C., YU H., HE J., WANG C.J. Photo-generated hydroxyl radicals contribute to the formation of halogen radicals leading to ozone depletion on and within polar stratospheric clouds surface. Chemosphere, **291** (1), 132816, **2022**.

29. ZOU X.D., CAI F., WANG X.Y., LI K.F., ZHANG Y.H., WANG H.Y., YANG H.B., LIU Y.C. Study on the change of ozone concentration in Liaoning province. Ecology and Environmental Sciences, **29** (9), 1830, **2020**.

30. WEI J., LI Z.Q., WANG J., LI C., GUPTA P., CRIBB M. Ground-level gaseous pollutants (NO_2, SO_2, and CO) in China: daily seamless mapping and spatiotemporal variations. Atmospheric Chemistry and Physics, **23** (2), 1511, **2023**.

31. SHEN Y., JIANG F., FENG S.Z., ZHENG Y.H., CAI Z., LYU X.P. Impact of weather and emission changes on NO_2 concentrations in China during 2014-2019. Environmental Pollution, **269**, 116163, **2021**.

32. ZHANG X.R., XIAO X., WANG F., BRASSEUR G., CHEN S.Y., WANG J., GAO M. Observed sensitivities of $PM_{2.5}$ and O_3 extremes to meteorological conditions in China and implications for the future. Environment International, **168**, 107428, **2022**.

33. PERETTI M., PIÑEIRO G., LONG M.E.F., CARNELOS D.A. Influence of the precipitation interval on wet atmospheric deposition. Atmospheric Environment, **237**, 117580, **2020**.

34. YU B.Y., ZHAO G.P., AN R.Y. Framing the picture of energy consumption in China. Natural Hazards, **99** (3), 1469, **2019**.